A DC-AC INVERTER-INDUCTION MOTOR SYSTEM NETWORK MODEL COMPATIBLE WITH COMMONLY KNOWN NETWORK ANALYSIS SOFTWARE PACKAGES

A.A. Arkadan
Marquette University
Milwaukee Wisconsin

V. Rossillo-Johnson N.A. Demerdash
Clarkson University
Potsdam New York

ABSTRACT

A method for modeling electronically commutated inverter fed induction motor systems is presented. The machine equivalent network model was derived from the application of Park's dq0 transformation to the differential equations governing the dynamics of the induction motor. The method resulted in an equivalent system network model which is compatible with most commonly known network analysis software packages. The method was used in the simulation of the dynamic steady state performance of a 204 V, 3 phase, 60 Hz, 1/3 hp, 4 pole induction motor-inverter system. The system was tested in the laboratory, under various load conditions. A comparison between the simulated and test results revealed a good agreement between the two sets of data. Furthermore, the model was used in the evaluation of the effects of 180° and 120° electrical inverter conduction periods on the performance of such inverter-machine system.

INTRODUCTION

Models for the analysis and prediction of the performance of rotating electric machinery interfaced with electronic power conditioning systems can be found throughout the recent literature. A sample of such work is references [1] through [4]. In such machine systems which include ac as well as dc conventional rotating machines, switching is continuously taking place in the external power conditioning components connected to the machine. Furthermore, the corresponding network topologies of these systems are undergoing continuous and cyclical changes. The continuous switching of the associated conditioning components results in time harmonics in the current and voltage waveforms. This means that these current and voltage waveforms are not of a sinusoidal or simple rectangular nature. Accordingly, the modeling method should account for these harmonics resulting from the continuous topological changes in the system equivalent network model. Application of steady state and frequency domain network analysis methods or dc circuit analysis methods will often lead to misleading results. Accordingly, one should use the differential equations governing the dynamics of such systems. In previous investigations such as those of references [1,2], the machine system network models were tailored to fit specific applications. However, in reference [3], a more general network analysis approach was presented and was applied to electronically commutated brushless dc motors, and in reference [4], a generic-type network modeling approach was applied to a synchronous generator feeding rectified loads.

In this work, a model for the analysis of the dynamic steady state performance of electronically commutated inverter fed induction motor systems is presented. Implementation of the solution of the network model was carried out using a standard software package for network analysis, SPICE, version 2G.6 [5]. The machine network model was derived from the application of the dq0 Park's transformation to the differential equations governing the dynamics of the induction motor. Steps of the model development are given in the paper. The validity of the developed model was confirmed by applying it to the simulation of the steady state performance of a practical example. A comparison between the numerical solutions and corresponding experimental data at different load conditions on the same system is given in the paper.

MACHINE SYSTEM NETWORK MODEL

A schematic of the inverter fed induction motor system is given in Figure (1). The idealized induction motor is represented schematically by the coils shown in Figure (2). Here, the stator three phases are represented by the coils (A), (B), and (C), and the rotor phases are represented by the coils (a), (b), and (c). The three stator phase windings, as well as the three rotor phase windings of the machine are assumed to be sinusoidally distributed. That is, each winding produces a sinusoidally distributed mmf in the air gap. The angular position of the rotor, σ, is defined as the angle between the A-axis of the stator and

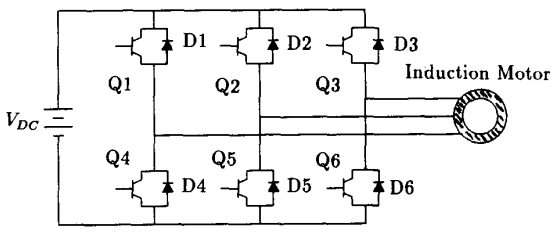

Figure (1): SCHEMATIC OF INVERTER-FED INDUCTION MOTOR SYSTEM

CH2719-3/89/0000-0195 $1.00 © 1989 IEEE

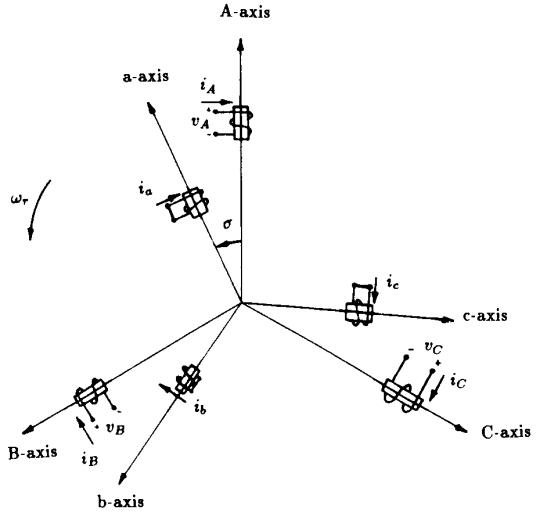

Figure (2): SCHEMATIC OF THE INDUCTION MOTOR WINDINGS

the a-axis of the rotor at any instant of time. The differential equations governing the dynamics of the induction motor in the abc frame of reference are as follows :

$$\left[\begin{array}{c} v_A \\ v_B \\ v_C \\ \hline v_a \\ v_b \\ v_c \end{array}\right] = \left[\begin{array}{ccc|ccc} r_A & 0 & 0 & 0 & 0 & 0 \\ 0 & r_B & 0 & 0 & 0 & 0 \\ 0 & 0 & r_C & 0 & 0 & 0 \\ \hline 0 & 0 & 0 & r_a & 0 & 0 \\ 0 & 0 & 0 & 0 & r_b & 0 \\ 0 & 0 & 0 & 0 & 0 & r_c \end{array}\right] \left[\begin{array}{c} i_A \\ i_B \\ i_C \\ \hline i_a \\ i_b \\ i_c \end{array}\right]$$

$$+ \left[\begin{array}{ccc|ccc} L_{AA} & L_{AB} & L_{AC} & L_{Aa} & L_{Ab} & L_{Ac} \\ L_{BA} & L_{BB} & L_{BC} & L_{Ba} & L_{Bb} & L_{Bc} \\ L_{CA} & L_{CB} & L_{CC} & L_{Ca} & L_{Cb} & L_{Cc} \\ \hline L_{aA} & L_{aB} & L_{aC} & L_{aa} & L_{ab} & L_{ac} \\ L_{bA} & L_{bB} & L_{bC} & L_{ba} & L_{bb} & L_{bc} \\ L_{cA} & L_{cB} & L_{cC} & L_{ca} & L_{cb} & L_{cc} \end{array}\right] \frac{d}{dt} \left[\begin{array}{c} i_A \\ i_B \\ i_C \\ \hline i_a \\ i_b \\ i_c \end{array}\right]$$

$$+ \omega_r \left\{ \frac{d}{d\sigma} \left[\begin{array}{ccc|ccc} L_{AA} & L_{AB} & L_{AC} & L_{Aa} & L_{Ab} & L_{Ac} \\ L_{BA} & L_{BB} & L_{BC} & L_{Ba} & L_{Bb} & L_{Bc} \\ L_{CA} & L_{CB} & L_{CC} & L_{Ca} & L_{Cb} & L_{Cc} \\ \hline L_{aA} & L_{aB} & L_{aC} & L_{aa} & L_{ab} & L_{ac} \\ L_{bA} & L_{bB} & L_{bC} & L_{ba} & L_{bb} & L_{bc} \\ L_{cA} & L_{cB} & L_{cC} & L_{ca} & L_{cb} & L_{cc} \end{array}\right] \left[\begin{array}{c} i_A \\ i_B \\ i_C \\ \hline i_a \\ i_b \\ i_c \end{array}\right] \right\} \quad (1)$$

where $\omega_r = \dot{\sigma}$ is the instantaneous rotor speed in electrical rad/s, and is related to the synchronous speed ω_s, which is also in electrical rad/s, and to the per unit slip s as follows:

$$\omega_r = (1 - s)\omega_s \quad (2)$$

In equation (1), two similar subscripts of the letter L denote a self inductance of a winding, and two different subscripts denote a mutual inductance between two windings. Furthermore, the first right hand term of equation (1) represents the ohmic voltage drop in the machine windings, the second term represents the transformer voltage components, and the last term represents the rotational voltage components.

For an idealized conventional induction machine, because of the cylindrical nature of the rotor geometry, the flux paths for the three phase windings of the stator are identical and independent of the rotor position. Accordingly, the self and mutual inductances of the stator are equal and independent of rotor position. That is, one can write the following [6]:

$$L_{AA} = L_{BB} = L_{CC} = L_{ss} \quad (3)$$

$$L_{AB} = L_{BC} = L_{CA} = L_{sm} \quad (4)$$

A similar reasoning can be applied to rotor self and mutual inductances, which accordingly can be expressed as follows:

$$L_{aa} = L_{bb} = L_{cc} = L_{rr} \quad (5)$$

$$L_{ab} = L_{bc} = L_{ca} = L_{rm} \quad (6)$$

Also, since we are dealing with a three phase balanced machine, the rotor and stator resistances are as follows:

$$r_A = r_B = r_C = r_s \quad (7)$$

$$r_a = r_b = r_c = r_r \quad (8)$$

In the case of the mutual inductances between the stator and rotor windings, these mutual inductances are functions of the angular position, σ, of the rotor windings with respect to the stator windings. Therefore, these mutual inductances can be expressed as follows [6]:

$$L_{Aa} = L_{Bb} = L_{Cc} = L_{srm}cos(\sigma) \quad (9)$$

$$L_{Ab} = L_{Bc} = L_{Ca} = L_{srm}cos(\sigma + 2\pi/3) \quad (10)$$

$$L_{Ac} = L_{Ba} = L_{Cb} = L_{srm}cos(\sigma + 4\pi/3) \quad (11)$$

In order to eliminate the dependence of the inductances in equations (9) through (11), on the rotor angle, σ, the practice of transformation to a dq0 frame of reference is widely accepted by machine analysts and designers, and can be found throughout the literature.This transformation approach is adopted here, and a frame of reference fixed to the rotor is used [6-8].

TRANSFORMATION OF abc MODEL TO dq0 FRAME OF REFERENCE

The differential equations governing the dynamics of the induction motor in the abc frame of reference, equation (1), can be expressed in compact matrix form as follows:

$$\left[\begin{array}{c} \underline{V}_{ABC} \\ \hline \underline{V}_{abc} \end{array}\right] = \left[\begin{array}{c|c} \underline{\mathcal{R}}_{ss} & \underline{0} \\ \hline \underline{0} & \underline{\mathcal{R}}_{rr} \end{array}\right] \left[\begin{array}{c} \underline{I}_{ABC} \\ \hline \underline{I}_{abc} \end{array}\right] +$$

$$\left[\begin{array}{c|c} \underline{\mathcal{L}}_{ss} & \underline{\mathcal{L}}_{sr} \\ \hline \underline{\mathcal{L}}_{sr}^t & \underline{\mathcal{L}}_{rr} \end{array}\right] \frac{d}{dt} \left[\begin{array}{c} \underline{I}_{ABC} \\ \hline \underline{I}_{abc} \end{array}\right] + \omega_r \frac{d}{d\sigma} \left[\begin{array}{c|c} \underline{\mathcal{L}}_{ss} & \underline{\mathcal{L}}_{sr} \\ \hline \underline{\mathcal{L}}_{sr}^t & \underline{\mathcal{L}}_{rr} \end{array}\right] \left[\begin{array}{c} \underline{I}_{ABC} \\ \hline \underline{I}_{abc} \end{array}\right] \quad (12)$$

where the superscript t denotes a transpose of a matrix.

In order to get rid of the dependence of the various inductance terms in equation (1), the Park's dq0 transformation with a frame of reference fixed to the rotor was adopted [6-8], such that:

$$\underline{I}_{DQ0} = \underline{T}_s \cdot \underline{I}_{ABC} \quad ; \quad \underline{I}_{ABC} = \underline{T}_s^{-1} \cdot \underline{I}_{DQ0} \quad (13)$$

$$\underline{V}_{DQ0} = \underline{T}_s \cdot \underline{V}_{ABC} \quad ; \quad \underline{V}_{ABC} = \underline{T}_s^{-1} \cdot \underline{V}_{DQ0} \tag{14}$$

$$\underline{I}_{dqo} = \underline{T}_r \cdot \underline{I}_{abc} \quad ; \quad \underline{I}_{abc} = \underline{T}_r^{-1} \cdot \underline{I}_{dqo} \tag{15}$$

$$\underline{V}_{dqo} = \underline{T}_r \cdot \underline{V}_{abc} \quad ; \quad \underline{V}_{abc} = \underline{T}_r^{-1} \cdot \underline{V}_{dqo} \tag{16}$$

where

$$\underline{T}_s = 2/3 \begin{bmatrix} cos(\sigma) & cos(\sigma - 2\pi/3) & cos(\sigma - 4\pi/3) \\ -sin(\sigma) & -sin(\sigma - 2\pi/3) & -sin(\sigma - 4\pi/3) \\ 1/2 & 1/2 & 1/2 \end{bmatrix} \tag{17}$$

and

$$\underline{T}_r = 2/3 \begin{bmatrix} 1 & -1/2 & -1/2 \\ 0 & \sqrt{3}/2 & -\sqrt{3}/2 \\ 1/2 & 1/2 & 1/2 \end{bmatrix} \tag{18}$$

Applying this transformation to equation (1) yields the following state equations which govern the dynamics of the induction motor in the dq0 frame of reference:

$$\left[\begin{array}{c} \underline{V}_{DQ0} \\ \hline \underline{V}_{dqo} \end{array}\right] = \left[\begin{array}{c|c} \underline{\mathcal{R}}_{ss} & \underline{0} \\ \hline \underline{0} & \underline{\mathcal{R}}_{rr} \end{array}\right] \left[\begin{array}{c} \underline{I}_{DQ0} \\ \hline \underline{I}_{dqo} \end{array}\right]$$

$$+ \left[\begin{array}{c|c} \underline{\mathcal{L}}_1 & \underline{\mathcal{L}}_2 \\ \hline \underline{\mathcal{L}}_2 & \underline{\mathcal{L}}_3 \end{array}\right] \frac{d}{dt} \left[\begin{array}{c} \underline{I}_{DQ0} \\ \hline \underline{I}_{dqo} \end{array}\right] + \omega_r \left[\begin{array}{c|c} \underline{\mathcal{L}}_4 & \underline{\mathcal{L}}_5 \\ \hline \underline{0} & \underline{0} \end{array}\right] \left[\begin{array}{c} \underline{I}_{DQ0} \\ \hline \underline{I}_{dqo} \end{array}\right] \tag{19}$$

where

$$\underline{\mathcal{L}}_1 = \begin{bmatrix} (L_{ss} - L_{sm}) & 0 & 0 \\ 0 & (L_{ss} - L_{sm}) & 0 \\ 0 & 0 & (L_{ss} + 2L_{sm}) \end{bmatrix},$$

$$\underline{\mathcal{L}}_2 = \begin{bmatrix} 1.5L_{srm} & 0 & 0 \\ 0 & 1.5L_{srm} & 0 \\ 0 & 0 & 0 \end{bmatrix},$$

$$\underline{\mathcal{L}}_3 = \begin{bmatrix} (L_{rr} - L_{rm}) & 0 & 0 \\ 0 & (L_{rr} - L_{rm}) & 0 \\ 0 & 0 & (L_{rr} + 2L_{rm}) \end{bmatrix},$$

$$\underline{\mathcal{L}}_4 = \begin{bmatrix} 0 & -(L_{ss} - L_{sm}) & 0 \\ (L_{ss} - L_{sm}) & 0 & 0 \\ 0 & 0 & 0 \end{bmatrix}, \text{ and}$$

$$\underline{\mathcal{L}}_5 = \begin{bmatrix} 0 & -1.5L_{srm} & 0 \\ 1.5L_{srm} & 0 & 0 \\ 0 & 0 & 0 \end{bmatrix}$$

Here,

- $\underline{I}_{DQ0}$ is the array of the direct, quadrature, and zero sequence components of the current in the stator,
- $\underline{V}_{DQ0}$ is the array of the direct, quadrature, and zero sequence components of the voltage at the stator terminals,
- $\underline{I}_{dqo}$ is the array of the direct, quadrature, and zero sequence components of the current in the rotor,
- $\underline{V}_{dqo}$ is the array of the direct, quadrature, and zero sequence components of the voltage at the rotor terminals,
- L_{ss} is the stator self inductance per phase in H,
- L_{sm} is the mutual inductance between two stator phases in H,
- L_{srm} is the mutual inductance between a stator phase and a rotor phase in H,
- L_{rr} is the rotor self inductance per phase in H,
- L_{rm} is the mutual inductance between two rotor phases in H,
- r_s is the stator phase resistance in Ω, and
- r_r is the rotor phase resistance in Ω.

The relationships between these inductances and resistances and those obtained from no-load and blocked rotor tests on an induction machine can be found in references [8-10]. Furthermore, the developed electromagnetic torque can be obtained for a three phase machine from dq0 quantities as follows [10]:

$$T_{em} = \frac{9}{8} P L_{srm} (i_Q i_d - i_D i_q) \tag{20}$$

where P is the number of poles.

For balanced steady state conditions, the zero sequence voltages and currents are zero. Accordingly, the equivalent network representation of the state model given by equation (19) is given by Figure (3). The resistances, self and mutual inductances, and the independent voltage sources in Figure (3) are self explanatory. The current controlled voltage sources are the diamond shaped elements and are expressed as follows:

$$f_1(i_Q) = \omega_r (L_{ss} - L_{sm}) i_Q \tag{21}$$

$$f_2(i_q) = 1.5 \omega_r L_{srm} i_q \tag{22}$$

$$f_3(i_D) = -\omega_r (L_{ss} - L_{sm}) i_D \tag{23}$$

$$f_4(i_d) = -1.5 \omega_r L_{srm} i_d \tag{24}$$

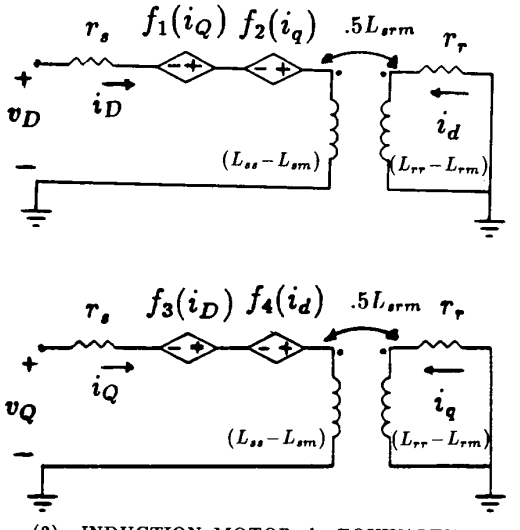

Figure (3): INDUCTION MOTOR dq EQUIVALENT NETWORK MODEL

Writing the loop equations for the equivalent network of Figure(3), one would obtain a set of equations which are identical to the state model of equation (1) after adding the zero sequence equations. Again, for balanced steady state conditions the zero sequence currents and voltages are zero. Hence, the network model of Figure (3) is a full representation of the machine's state model of equation (19). The dynamics of this network are identical to the dynamics of the induction machine, subject to the external constraints and initial load conditions. The external constraints are stemming from the states of the external power conditioning components (inverter) connected to the machine terminals.

The inverter currents and voltages are in the physical abc frame of reference rather than the non-physical dq0 frame of reference. Therefore a way must be found to link the induction machine equivalent network model developed above, Figure (3), to the actual inverter network. The linking of the dq network model of the induction machine to the abc inverter network is given below.

Consider the induction machine stator currents i_D, and i_Q, shown in Figure (3). These currents can be expressed in terms of the inverter currents, i_A, i_B, and i_C, as follows:

$$i_D = \frac{2}{3}[i_A cos(\omega_r t) + i_B cos(\omega_r t - 2\pi/3) + i_C cos(\omega_r t - 4\pi/3)] \quad (25)$$

$$i_Q = -\frac{2}{3}[i_A sin(\omega_r t) + i_B sin(\omega_r t - 2\pi/3) + i_C sin(\omega_r t - 4\pi/3)] \quad (26)$$

Furthermore, the inverter terminal voltages v_A, v_B, and v_C can be expressed in terms of the machine terminal voltages v_D and v_Q, shown in Figure (3), as follows:

$$v_A = v_D cos(\omega_r t) - v_Q sin(\omega_r t) \quad (27)$$

$$v_B = v_D cos(\omega_r t - 2\pi/3) - v_Q sin(\omega_r t - 2\pi/3) \quad (28)$$

$$v_C = v_D cos(\omega_r t - 4\pi/3) - v_Q sin(\omega_r t - 4\pi/3) \quad (29)$$

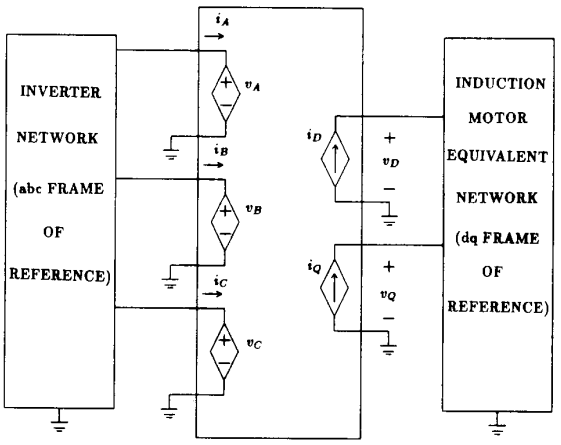

Figure (4): CIRCUIT ELEMENTS LINKING THE INDUCTION MOTOR dq FRAME CURRENTS AND VOLTAGES TO THE INVERTER abc FRAME CURRENTS AND VOLTAGES

Accordingly, based on equations (25) through (29), the voltages v_A, v_B, and v_C can be represented as voltage controlled voltage sources, and the stator currents i_D and i_Q can be represented as current controlled current sources in a network model. This resulted in the sought network link between the machine network model in the dq frame of reference and the inverter network model in the abc frame of reference as shown in Figure (4). As a result, the induction machine's equivalent network model, and the inverter's network model can be merged together to yield the global network model shown in Figure (5).

The simulation of the dynamics of this type of network, Figure (5), can be implemented using the majority of commonly available network analysis software packages. In this work, the network analysis software package 'SPICE' version 2G.6 [5], was used in the simulation given in this paper.

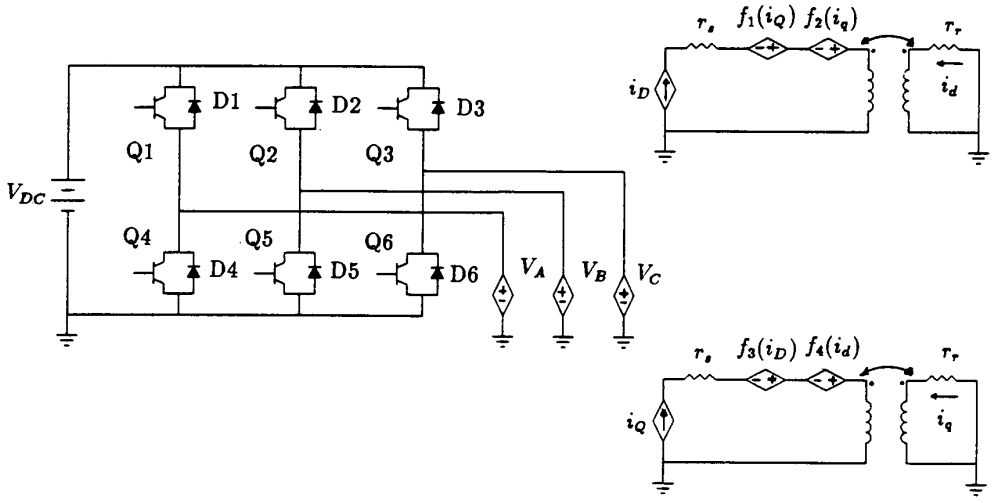

Figure (5): EQUIVALENT NETWORK MODEL OF INVERTER-INDUCTION MOTOR SYSTEM

SYSTEM MODEL APPLICATIONS AND EXPERIMENTAL VERIFICATION

The inverter-fed-induction-motor system model of Figure (5) above, was used to simulate the steady state dynamic performance of the 240 V, 3 phase, 60 Hz, 1/3 hp, 4 pole induction motor-inverter system at different load conditions with an inverter conduction period of 180° electrical. The system was physically set up in the laboratory for test purposes in order to check the validity of the simulation results versus actual performance results. The inverter fed induction motor system test setup and instrumentations are shown in Figure (6). The system was operated and tested at two load conditions. These load conditions are given in Table (1). The two load conditions were also simulated using SPICE and the system global network model of Figure (5). The system performance results under these load conditions as obtained from the experimental setup and the simulation model are compared next in the paper.

Simulation and Experimental Results of Test Run # 1:

A summary of test and simulated values of the inverter fed induction motor system phase current, line-to-line voltage, and torque is given in Table (2) for the conditions of test #1, see Table (1). It is obvious from these results that the simulated voltage, current, and torque values are in very good agreement with the test results.

For this test condition, the oscillogram of the stator phase current is given in Figure (7), while the corresponding computer simulated waveform (CSWF) of this current is given in Figure (8). Meanwhile, the oscillogram and the CSWF of the stator line to line terminal voltage are given in Figures (9) and (10) respectively. A comparison between both oscillograms and their corresponding CSWFs reveals a very good agreement between the profiles of the actual currents and voltages and the profiles of the corresponding simulated ones. The simulated torque profile is given in Figure (11). Notice that this profile as well as the other torque profiles given in this paper contain an initial transient. This is due to the nature of SPICE and due to fact that the dynamic equation of motion is not included in the model. Hence the early part of a torque profile given in this paper has no physical significance. However, one is interested in the steady state behavior of the torque, as mentioned earlier, and that is displayed accurately in the later part of a profile. The average of the steady state part of the simulated torque profile given in Figure (11) was found to be 0.7 N.m., and is in good agreement with the measured value of 0.66 N.m., see Table (2).

Test No.	Frequency of Inverter Hz	Rotor Speed r/min	V_{DC} Volts
#1	60	1750	188.5
#2	60	1730	188.5

Table 1: INVERTER-MOTOR SYSTEM TEST CONDITIONS

Quantity	Actual	Predicted
Phase Current (Amps Peak)	1.7	1.6
Line to Line Voltage (Volts Peak)	185.0	188.5
Torque (N-m Average)	0.66	0.7

Table 2: COMPARISON BETWEEN ACTUAL AND SIMULATED RESULTS (TEST #1)

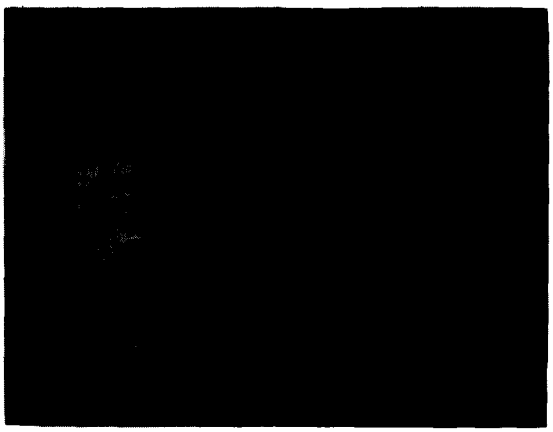

Figure (6): INVERTER-INDUCTION MOTOR SYSTEM TEST SETUP

Figure (7): OSCILLOGRAM OF MACHINE PHASE CURRENT, TEST #1: ROTOR SPEED=1750 r/min. (Horizontal: 5ms/div. Vertical 1 A/div.), 1.7 A peak

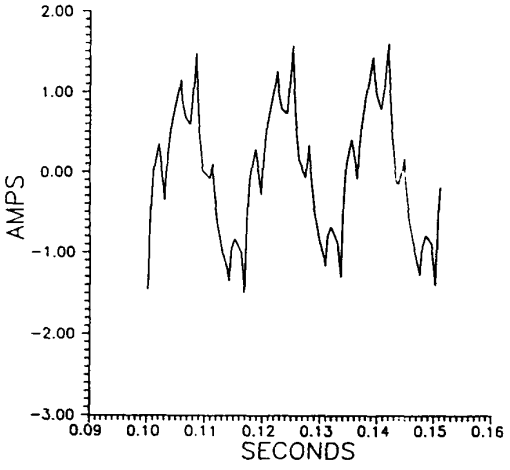

Figure (8): CSWF OF MACHINE PHASE CURRENT, TEST #1: ROTOR SPEED=1750 r/min.

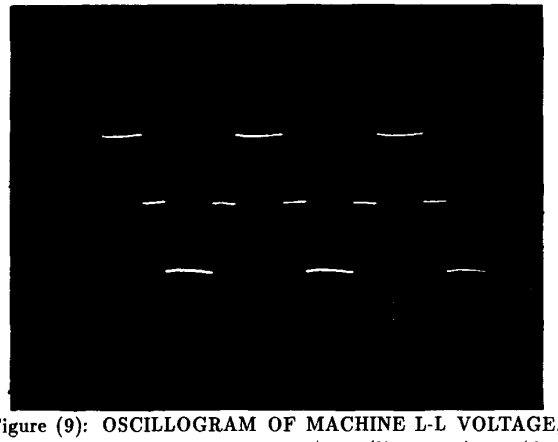

Figure (9): OSCILLOGRAM OF MACHINE L-L VOLTAGE, TEST #1: ROTOR SPEED=1750 r/min. (Horizontal: 5ms/div. Vertical 100 V/div.), 185 V peak

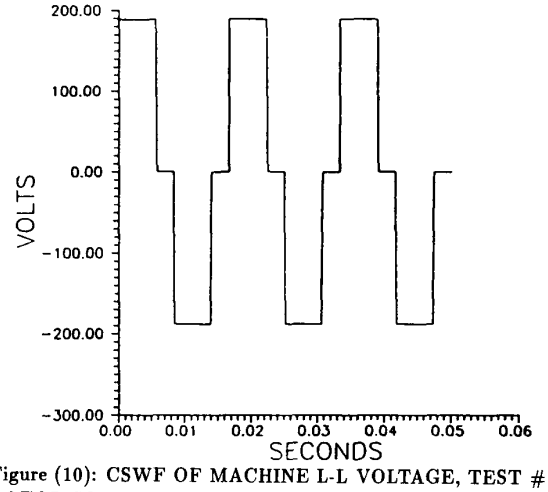

Figure (10): CSWF OF MACHINE L-L VOLTAGE, TEST #1: ROTOR SPEED=1750 r/min.

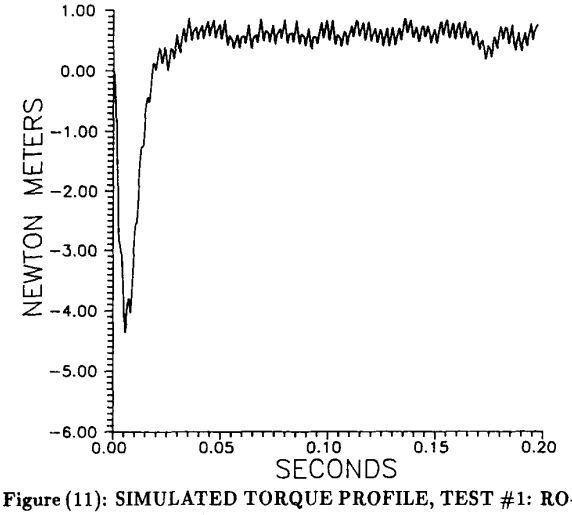

Figure (11): SIMULATED TORQUE PROFILE, TEST #1: ROTOR SPEED=1750 r/min.

Simulation and Experimental Results of Test Run # 2:

A summary of test and simulated values of the inverter fed induction motor system phase current, line-to-line voltage, and torque is given in Table (3) for the conditions of test #2, see Table (1). Again, it is obvious from these results that the simulated voltage, current, and torque values are in very good agreement with the test results.

For this test condition, the oscillogram of the stator phase current and its corresponding CSWF are given in Figures (12) and (13) respectively, Meanwhile, the oscillogram and the CSWF of the stator line to line terminal voltage are given in Figures (14) and (15) respectively. Again, a comparison between both oscillograms and their corresponding CSWFs reveals a very good agreement between the profiles of the actual currents and voltages and the profiles of the corresponding simulated ones. The simulated torque profile is given in Figure (16). The average of the steady state part of the simulated torque profile was found to be 0.9 N.m., and is in good agreement with the measured value of 0.85 N.m., see Table (3).

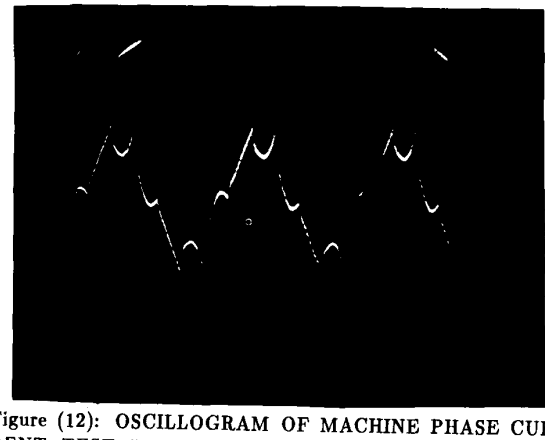

Figure (12): OSCILLOGRAM OF MACHINE PHASE CURRENT, TEST #2: ROTOR SPEED=1730 r/min. (Horizontal: 5ms/div. ; Vertical 1 A/div.), 1.8 A peak

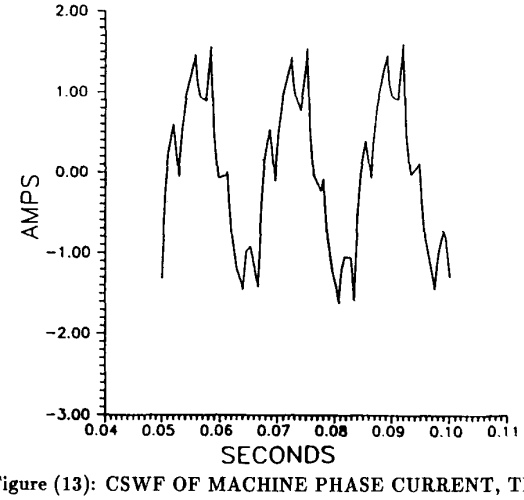

Figure (13): CSWF OF MACHINE PHASE CURRENT, TEST #1: ROTOR SPEED=1730 r/min.

Examination of the above simulated and test results for the induction motor-inverter system for conditions #1 and #2 of Table (1), demonstrates the validity of this modeling approach. Therefore, this modeling approach can be used to predict the performance of other inverter fed induction motor systems of different ratings. Accordingly, this approach was used to study effects of varying the inverter conduction period on the torque of a 15 hp induction motor driven by an inverter of similar circuit topology.

Quantity	Actual	Predicted
Phase Current (Amps Peak)	1.8	1.7
Line to Line Voltage (Volts Peak)	185.0	188.5
Torque (N-m Average)	0.85	0.9

Table 3: COMPARISON BETWEEN ACTUAL AND SIMULATED RESULTS (TEST #2)

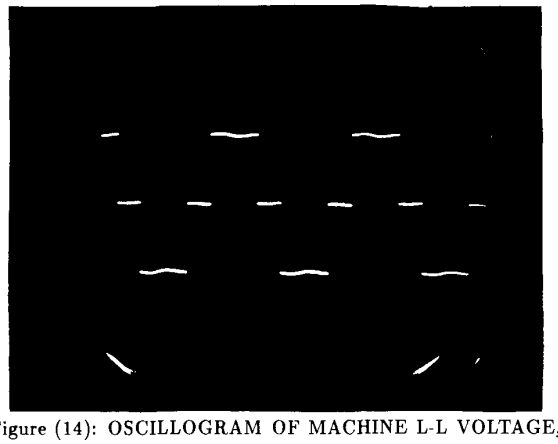

Figure (14): OSCILLOGRAM OF MACHINE L-L VOLTAGE, TEST #2: ROTOR SPEED=1730 r/min. (Horizontal: 5ms/div. Vertical 100 V/div.), 185 V peak

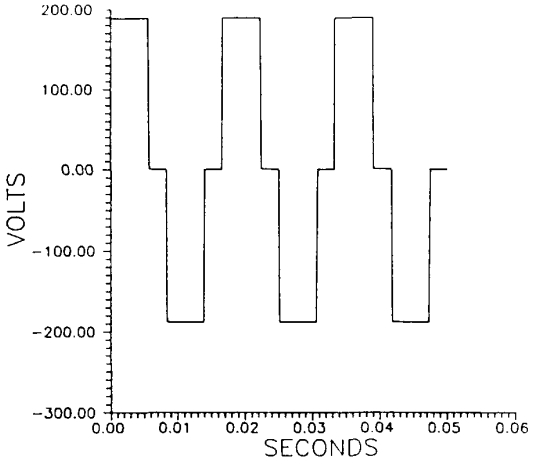

Figure (15): CSWF OF MACHINE L-L VOLTAGE, TEST #1: ROTOR SPEED=1730 r/min.

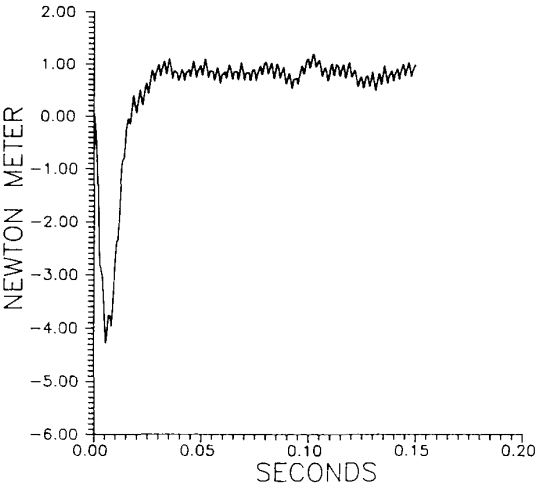

Figure (16): SIMULATED TORQUE PROFILE, TEST #2: ROTOR SPEED=1730 r/min.

Use of Model in Studying Effects of Inverter Conduction Period on Developed Torque:

An important element from the point of view of system performance is the permissible conduction period of the six transistors of the inverter, Figure (1). Although this conduction period can be fixed to any interval ranging from less than 90° e to 180° e, it is particularly advantageous to fix the interval of conduction of the transistors at either 120° e or 180° e [2]. For this reason, the inverter fed induction motor model presented in this paper, was used to study the effects of 120° e and 180° e inverter conduction periods on the developed torque. The switching sequence of the inverter's transistors of 120° e and 180° e are given in Figures (17) and (18), respectively. The simulation for the two conduction periods was performed on an inverter fed 15 hp, 440 V, 3 phase, 60 Hz, 8 pole, wound rotor induction motor at a rotor speed of 810 r/min (slip=0.1).

By using the model developed here, it was found that in order for the 15 hp motor to develop a torque of 240 N.m.for the case of 180° e conduction period and a rotor speed of 810 r/min, a dc supply of 564 V was required. Meanwhile, for the case of 120° e conduction period and the same rotor speed of 810 r/min, a dc supply of 651 V was required to develop the same torque. Although it is the fundamental component of the inverter output voltage that is primarily responsible for the production of output torque, the harmonics also play a role in the characteristic of the torque pulsation and hence the overall torque profile. Accordingly, the inverter output voltage was Fourier analyzed for the two conduction periods to study the ratio of fundamental to harmonics. As expected, the ratio of the fundamental to the harmonics of the inverter terminal voltage was found to be higher for the 120° e conduction case [10]. This leads one to expect a smoother torque for the case of the 120° e conduction period. This was confirmed by the torque pulsations and profiles of the

two cases. The resulting torque profiles for the 180° e and 120° e conduction periods are given in Figures (19) and (20), respectively. Examination of the torque ripple for both cases, Table (4), reveals that the torque ripple is significantly higher for the 180° e case as compared to the 120° e case, as expected. These results further confirm the validity of the developed model. Thus, this modeling approach which takes into consideration the time harmonics resulting from the continuous switching of the associated power conditioning components can be used in predicting the performance characteristics such as torque profiles and associated noise problems which exist in such drive systems.

Comparison of Torque Ripple			
Conduction Case	V_{DC} (Volts)	Magnitude of Ripple (N.m.)	Average Torque (N.m.)
180° e	564	90.0	240.0
120° e	651	62.5	240.0

Table 4: COMPARISON OF TORQUE RIPPLE FOR 120° e AND 120° e

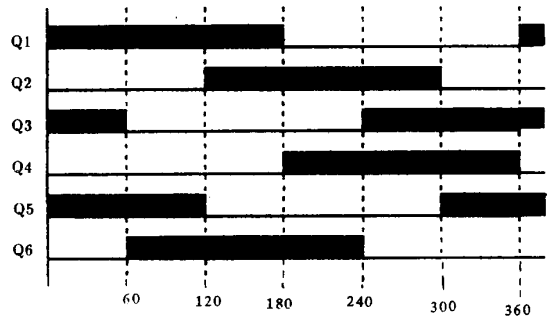

Figure (17): INVERTER SWITCHING SEQUENCE: 180° e CONDUCTION PERIOD

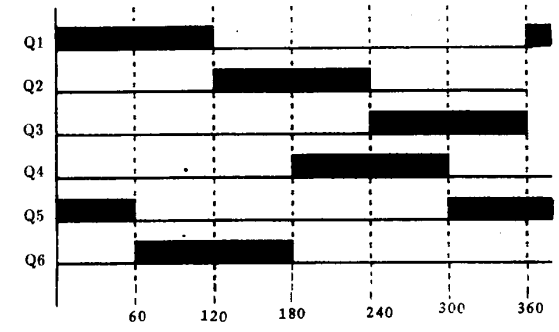

Figure (18): INVERTER SWITCHING SEQUENCE: 120° e CONDUCTION PERIOD

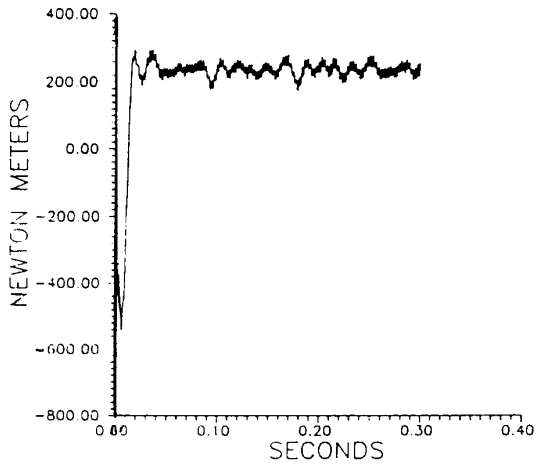

Figure (19): INVERTER DEVELOPED TORQUE PROFILE: 180° e CONDUCTION PERIOD

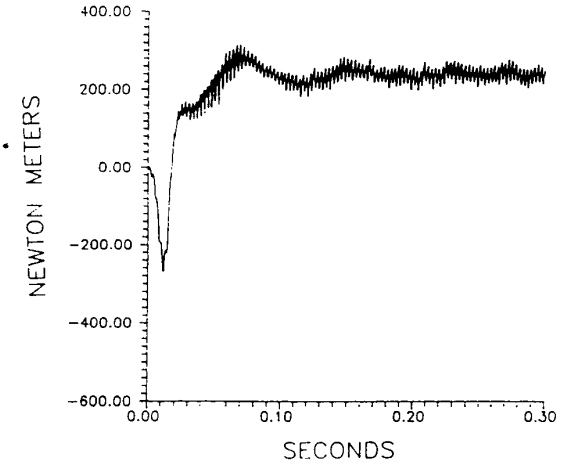

Figure (20): INVERTER DEVELOPED TORQUE PROFILE: 120° e CONDUCTION PERIOD

CONCLUSIONS

A method for modeling electronically commutated inverter fed induction motor systems was presented. The method resulted in an equivalent network model compatible with most commonly known network analysis software packages. The method was implemented in conjunction with SPICE Version 2G.6 network analysis software package in a computer program to simulate the performance of a 204 V, 60 Hz, 1/3 hp, 4 pole induction motor-inverter system. The simulation results were compared with actual experimental load runs on the same system. The good agreement between the simulated and test results given in this paper confirmed the validity of the model. This modeling

approach, which takes into consideration the time harmonics resulting from the continuous switching of the power conditioning components connected to the terminals of the machine, was used as well in studying effects of inverter conduction periods in the developed torque of a 440 V, 60 Hz, 15 hp, 8 pole induction motor-inverter system.

This modeling approach, besides being applicable to inverter fed induction motor systems, can be applied to other machines-power-conditioning systems. In future effort, the equation of motion as well as effects of space harmonics in the emfs and the machine inductances will be included in the analysis.

References

[1] Demerdash, N.A. and Nehl, T.W., "Dynamic Modeling of Brushless DC Motor For Aerospace Actuation", *IEEE Transactions on Aerospace and Electronic Systems,* Vol. AES-16, No. 6, pp. 811-821, 1980.

[2] Lipo, T.A. and Turnbull, F.G., "Analysis and Comparison of Two Types of Square Wave Inverter Drives", *IEEE Transactions on Industry Applications,* Vol. IA-11, No. 2, pp. 137-147, 1975.

[3] Nehl, T.W., Demerdash, N.A., Hijazi, T.M., and McHale, T.L., "Automatic Formulation of Models for Simulation of the Dynamic Performance of Electronically Commutated DC Machines", *IEEE Transactions on Power Apparatus and Systems,* Vol. PAS-104, No. 8, pp. 2214-2222, 1985.

[4] Arkadan, A.A., Hijazi, T.M., Demerdash, N.A., Vaidya, J.G., and Maddali, V.K., "Theoretical Development and Experimental Verification of a DC-AC Electronically Rectified Load-Generator System Model Compatible with common Network Analysis Software Packages", *IEEE Transactions on Energy Conversion,* Vol. EC-3, No. 1, pp.123-131, 1988.

[5] Vladimirescu, Zhang, Newton, Pederson, " SPICE Version 2G.6 Users Guide", Department of Electrical Enginneering and Computer Sciences, University of California, Berkeley.

[6] Fitzgerald, A.E., and Kingsly, C., *Electric Machinery,* Second Edition, McGraw- Hill Book Company, 1961.

[7] Concordia, C., *"Synchronous Machines Theory and Performance",* John Wiley & Sons, Inc., New York, 1951.

[8] Krause, P.C., and Thomas, C.H.,"Simulation of Symmetrical Induction Machinery",*IEEE Transactions on Power Apparatus and Systems,* Vol. PAS-84, No. 11, pp. 1038-1052, 1965.

[9] Veinott, C.G., *Theory and Design of Small Induction Motors,* McGraw-Hill Book Company, 1959.

[10] Rossillo-Johnson, V., "Time-Domain Equivalent Circuit Model for Analysis of Inverter-Fed Induction Motors Compatible with Common Network Analysis Software Packages", M.Sc. Thesis, *Clarkson University,* April 1987.